Surface instabilities and droplets formation in thin viscoelastic films

Valeria Barra[1], Shahriar Afkhami, Lou Kondic
Department of Mathematical Sciences, NJIT
[1] vb82@njit.edu

Introduction

This study is developed in the field of Computational Fluid Dynamics, focusing on thin films of viscoelastic liquids, such as polymeric fluids. The aim in this study is to give a full mathematical analysis and to provide numerical simulations for the moving interface of viscoelastic liquids. We are interested in the instabilities that cause the dewetting of the liquid on a solid substrate. Through our study we find that the viscoelastic physical parameters affect the dynamics of the instability as well as the final configuration of the fluid that reorganizes in blobs and droplets. We investigate how the formation of these droplets is affected by viscoelasticity, and we characterize them in number and size. Our findings are in agreement with the theoretical framework and have been verified through the tool of Linear Stability Analysis.

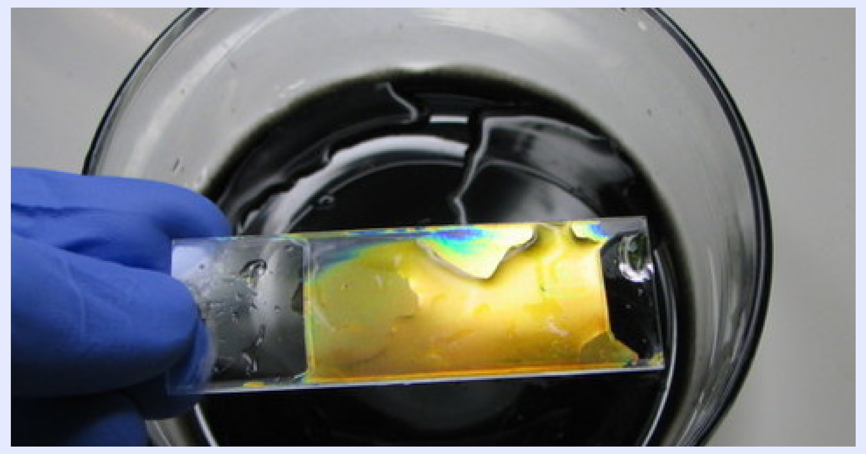

Figure 1: An application of a thin polymeric liquid film. Picture from www.foodproductiondaily.com - MIT research.

Governing Equations

The equation governing the hydrodynamics for the fluid interface of viscoelastic media is derived as a long-wave approximation of the conservation laws. The liquid is considered incompressible, with mass density ρ. The equation of conservation of mass and continuity of momentum are:

$$\nabla \cdot \mathbf{u} = 0\,, \quad \rho\left(\partial_t \mathbf{u} + \mathbf{u}\cdot\nabla\mathbf{u}\right) = -\nabla p_R + \nabla\cdot\tau\,, \tag{1}$$

where $\mathbf{u} = (u(x,y), v(x,y))$ is the velocity vector field, $\nabla = (\partial_x, \partial_y)$, and p_R the reduced pressure such that $p_R = p - \Pi$, where p is the hydrostatic pressure, while Π is the pressure induced by body forces of van der Waals type (attractive or repulsive). The stress tensor τ follows the Jeffreys model for viscoelastic fluids, which describes the non-Newtonian relation $\tau(\dot\gamma)$ between the stress tensor τ and the *strain rate* $\dot\gamma$:

$$\tau + \lambda_1\partial_t\tau = \eta(\dot\gamma + \lambda_2\partial_t\dot\gamma) \tag{2}$$

in which η is the shear viscosity coefficient and λ_1, λ_2 are, respectively, the *relaxation time* and the *retardation time* ($\lambda_1 \geq \lambda_2$). In figure 2 we can see a schematic of the fluid interface described parametrically by the function $y = h(x,t)$, where $y = 0$ is the solid substrate. At $y = 0$ we have Navier boundary conditions where $b \geq 0$ is the *slip length* ($b = 0$ means no slip, and $b \gg O(1)$ means strong-slip). We nondimensionalize these equations, using: $x = Lx^*$, $y = Hy^*$, $u = Uu^*$, $v = \varepsilon Uv^*$, $t = Tt^*$, with $T = L/U$, and $H/L = \varepsilon$, where ε is the small parameter, and the pressure is scaled as $PH/\eta U \sim \varepsilon^{-1}$. We derive the closed form equation for the interface of a thin layer of viscoelastic fluid (3). The full derivation can be found in [1].

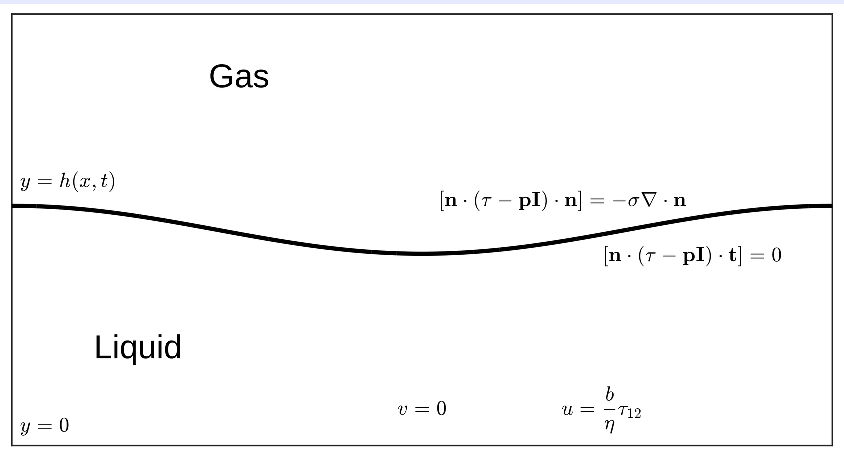

Figure 2: Scheme of the fluid interface and boundary conditions.

$$(1+\lambda_2\partial_t)h_t + (\lambda_2-\lambda_1)\frac{\partial}{\partial x}\left[\left(\frac{h^2}{2}\mathbf{Q} - h\mathbf{R}\right)h_t\right] = \frac{\partial}{\partial x}\left\{\left[(1+\lambda_1\partial_t)\frac{h^3}{3}\frac{\partial}{\partial x}p_R + (1+\lambda_2\partial_t)bh^2\frac{\partial}{\partial x}p_R\right]\right\}, \tag{3}$$

where Q and R satisfy respectively:

$$(1+\lambda_2\partial_t)Q = -\frac{\partial}{\partial x}(h_{xx} + \Pi(h))\,, \quad (1+\lambda_2\partial_t)R = -hh_{xxx} - h\Pi'(h)h_x \tag{4}$$

and the van der Waals potential is defined by: $\Pi(h) = \sigma(1-cos\theta)\left[(h_\star/h)^n - (h_\star/h)^m\right]/Mh_\star$,
with θ the contact angle with the substrate, $M = (n-m)/[(m-1)(n-1)]$ (with $n > m > 1$), $h_\star$ the precursor film thickness, and σ the surface tension.

Linear Stability Analysis

To study the film's response to a perturbation we consider $h = h_0 + \varepsilon h_0 e^{ikx+\omega t}$, where h_0 is the flat initial thickness, k the wave number $k = 2\pi/\lambda$, and ω the growth rate. Using these into equation (3) and keeping only terms up to $O(\varepsilon)$, we obtain the following disperion/dissipation relation:

$$\lambda_2\omega^2 + \left[1 + (k^4 - k^2\Pi'(h_0))\left(\lambda_1\frac{h_0^3}{3} + \lambda_2 bh_0^2\right)\right]\omega + (k^4 - k^2\Pi'(h_0))\left(\frac{h_0^3}{3} + bh_0^2\right) = 0\,. \tag{5}$$

Solving for the two roots of this quadratic equation we obtain one root strictly negative, let us say ω_2, and one root, say ω_1, with varying sign. The latter one is positive (unstable) for $-\sqrt{\Pi'(h_0)} < \omega_1 < \sqrt{\Pi'(h_0)}$.

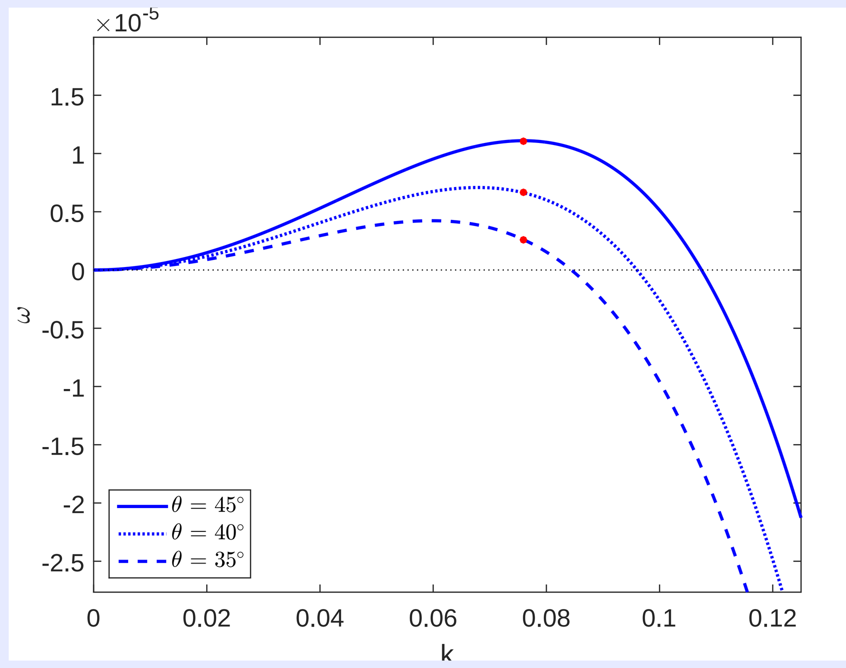

Figure 3: Linear Stability Analysis. The analytical growth rates (blue lines) are compared with our numerical simulations (red dots).

Results and Discussion

We numerically solve eq. (3) using Newton linearization of the non-linear terms, Crank-Nicolson scheme for the spacial derivatives and central finite differences for the second order derivative in time. The two ODEs for eq. (4) can be solved with any Euler method.

Dewetting Problem

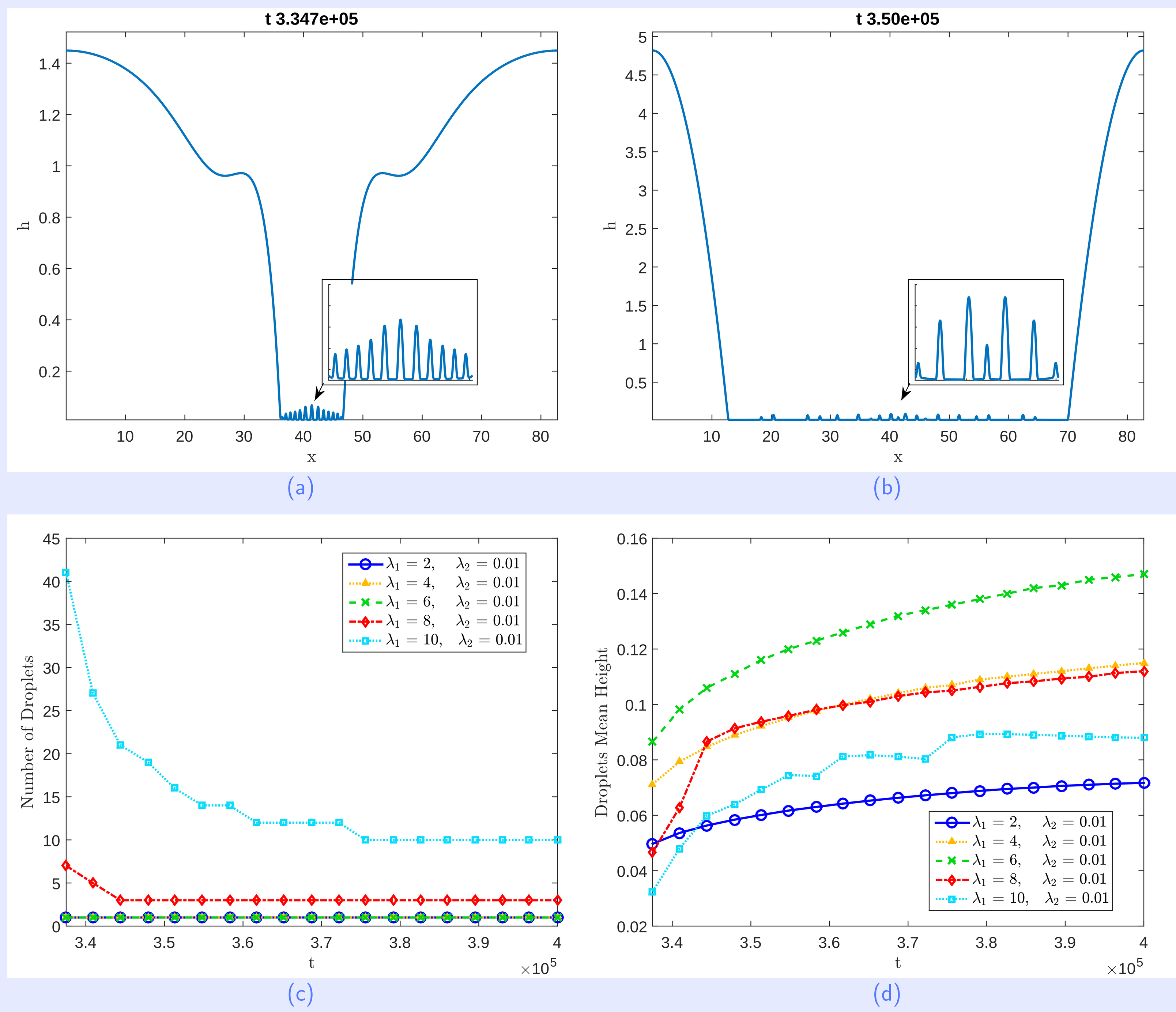

Figure 4: (a)-(b) Evolution for $h_0 = 1$ and $h_\star = 0.01$, $b = 0$, $\lambda_1 = 10$, $\lambda_2 = 0.01$ at two selected times. In (a) the unstable film separates in two rims and droplets form; these droplets stay until the final steady configuration in (b). In (c) number of droplets formed vs time, and in (d) mean droplets height vs time for five different values of λ_1.

Results and Discussion (cont'd)

In figures 4(a)-4(b) we see a numerical simulation of the evolution of the fluid interface. The unstable interface, initially flat, is perturbed, and it does not return to its initial profile, but it breaks up into two separate rims. The high elasticity of the fluid ($\lambda_1 = 10$) forms multiple wrinkles that lead to the formation of satellite droplets between the two major blobs of fluid (figure 4(a)). These droplets remain even when the fluid reaches the steady state final configuration (figure 4(b)). In 4(c)-4(d) the droplet analysis (in number and mean height) versus time, for five different values of λ_1.

Wetting Problem

We look at the spreading of a droplet on a solid substrate. The wetting of a droplet (or rivulet) of a Newtonian fluid on a solid substrate has been broadly studied in the past. We provide numerical simulations where we see the comparison of a Newtonian versus a non-Newtonian rivulet. We can see that the dynamics for the non-Newtonian front is faster initially (figure 5(b)), and that the two drops reach the steady configuration for large times (figure 5(d)).

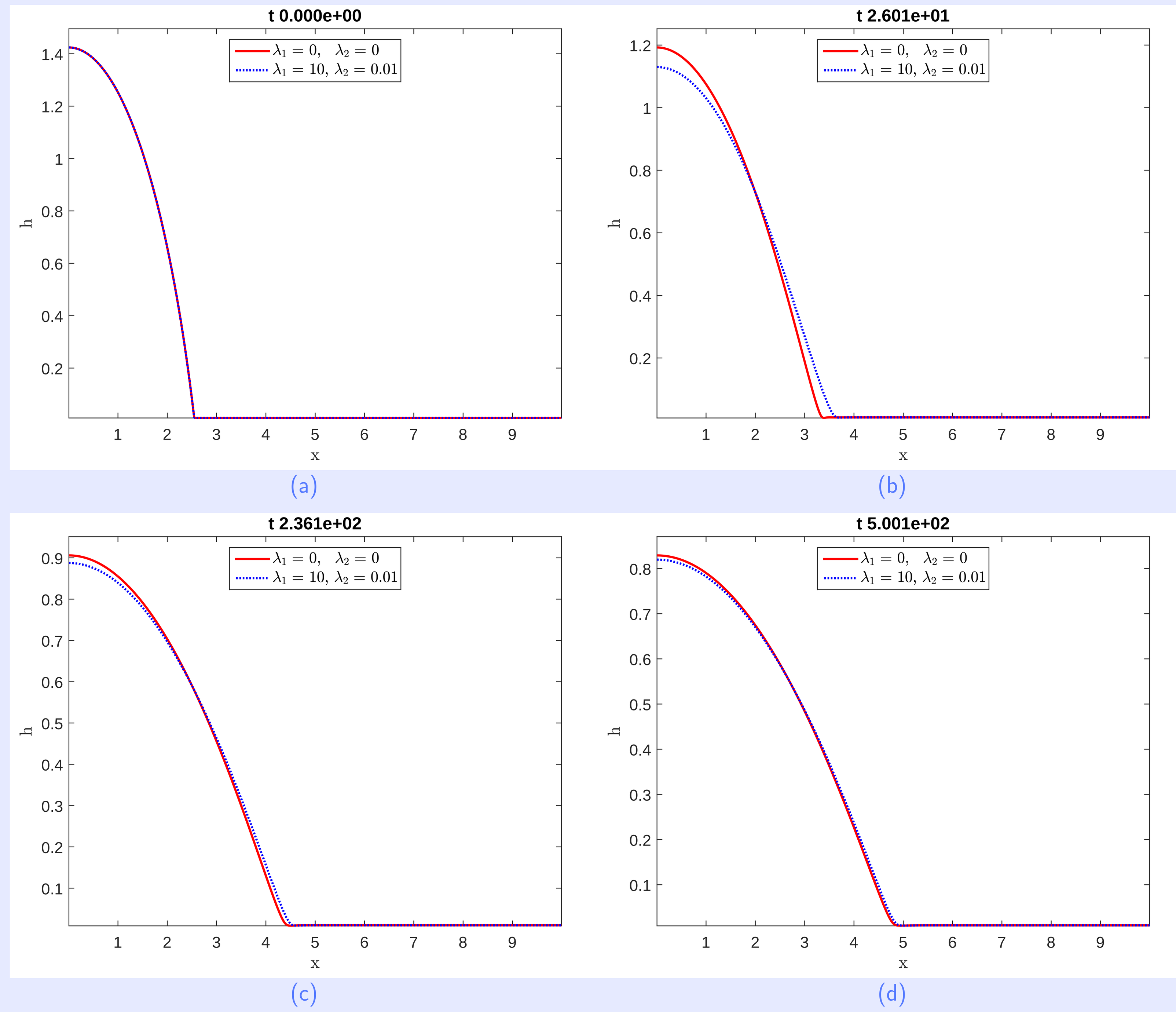

Figure 5: (a) Spreading of a Newtonian droplet ($\lambda_1 = \lambda_2 = 0$) vs a non-Newtonian one ($\lambda_1 = 10, \lambda_2 = 0.01$).

Conclusions and Future Work

Our numerical investigations allow to predict the dynamics of the moving interface of an unstable thin layer of polymeric liquid that dewets a solid substrate. Our findings are in agreement with the theoretical framework and have been verified through the tool of Linear Stability Analysis in the early times in which the fluid obeys the linear regime. We numerically solve the highly non-linear PDE governing the interface of the viscoelastic liquid, and our simulations show for the first time the formation of satellite droplets in thin films of viscoelastic fluids. We further analyzed and characterized the droplets in number, size and separation, depending on the physical parameters involved. We then looked at the wetting problem of a droplet of non-Newtonian fluid spreading on a solid substrate and compared it with the well-known case of a Newtonian liquid. This case leads to further investigations on the velocity of the moving contact line between the fluid interface and the solid substrate.

References

[1] Rauscher M., Münch A., Wagner B., Blossey R., *A thin-film equation for viscoelastic liquids of Jeffreys type*, Eur. Phys. J. E **17**, 373 – 379, (2005)

This work is partially supported by the NSF Grants No. DMS–1320037 & No. DMS–995904.